



## Structure and behavior of the barringerite Ni end-member, Ni<sub>2</sub>P, at deep Earth conditions and implications for natural Fe-Ni phosphides in planetary cores

Przemyslaw Dera,<sup>1</sup> Barbara Lavina,<sup>1</sup> Lauren A. Borkowski,<sup>2,3</sup> Vitali B. Prakapenka,<sup>1</sup> Stephen R. Sutton,<sup>1</sup> Mark L. Rivers,<sup>1</sup> Robert T. Downs,<sup>4</sup> Nabil Z. Boctor,<sup>5</sup> and Charles T. Prewitt<sup>4</sup>

Received 21 July 2008; revised 28 November 2008; accepted 18 December 2008; published 3 March 2009.

[1] High-pressure and high-temperature behavior of synthetic Ni<sub>2</sub>P has been studied in a laser-heated diamond anvil cell up to 50 GPa and 2200 K. Incongruent melting associated with formation of pyrite-type NiP<sub>2</sub> and amorphous Ni-P alloy was found at an intermediate pressure range, between 6.5 and 40 GPa. Above 40 GPa, Ni<sub>2</sub>P melts congruently. At room conditions, Ni<sub>2</sub>P has hexagonal C22-type structure, and without heating it remains in this structure to at least 50 GPa. With a bulk modulus  $K_0 = 201(8)$  GPa and  $K' = 4.2(6)$ , Ni<sub>2</sub>P is noticeably less compressible than hcp Fe, as well as all previously described iron phosphides, and its presence in the Earth core would favorably lower the core density. In contrast to Fe<sub>2</sub>P, the  $c/a$  ratio in Ni<sub>2</sub>P decreases on compression because of the lack of ferromagnetic interaction along the  $c$  direction. Lack of the C22→C23 transition in Ni<sub>2</sub>P rules out a stabilizing effect of Ni on the orthorhombic phase of natural (Fe<sub>1-x</sub>Ni<sub>x</sub>)<sub>2</sub>P allabogdanite.

**Citation:** Dera, P., B. Lavina, L. A. Borkowski, V. B. Prakapenka, S. R. Sutton, M. L. Rivers, R. T. Downs, N. Z. Boctor, and C. T. Prewitt (2009), Structure and behavior of the barringerite Ni end-member, Ni<sub>2</sub>P, at deep Earth conditions and implications for natural Fe-Ni phosphides in planetary cores, *J. Geophys. Res.*, 114, B03201, doi:10.1029/2008JB005944.

### 1. Introduction

[2] Our current knowledge about the chemical composition and physical properties of the deep interior of the Earth mostly comes from seismic observations, geophysical modeling, and high-pressure and high-temperature experiments constraining the properties and behavior of constituent minerals. Models of the Earth (1) make assumptions about the mineral phases present in the different layers of the interior; (2) utilize information about the experimentally determined crystal chemical trends, as well as the pressure and temperature evolution of physical properties of these materials; and (3) allow derivation of sound velocities, which can then be compared with seismic observations. It is now generally accepted that the density of the Earth core, estimated on the basis of seismic observations, is lower by about 10% than the density of pure iron at the  $P$  and  $T$  conditions of the core [Allegre *et al.*, 1995; Birch, 1952].

This density deficit can be explained by assuming the presence of light element alloys in the outer core. On the basis of the comparison of the silicate Earth model and cosmochemical abundances of elements, several prime candidates for the light element core constituents have been identified, including Si, S, O, C, N, H, and P [McDonough, 2003; McDonough and Sun, 1995]. Recently, an increasing number of mineral physics studies have been devoted to studying high-pressure and high-temperature phase relations and equations of state (EOS) of Fe-Ni-S-P minerals. While the estimates of the S and P content in the Earth core are not very high (2 and 0.2 wt %, respectively), S is suspected to be a major component of cores of other planetary bodies in the solar system, including Mars [see, e.g., Stewart *et al.*, 2007] and Mercury [Harder and Schubert, 2001; Stevenson *et al.*, 1983]. The Fe-S and Fe-P systems have very similar  $P$ - $T$  phase diagrams [Stewart and Schmidt, 2007], with major phases in the metal-rich part of the phase diagram representing stoichiometries of MB, M<sub>2</sub>B<sub>3</sub>, M<sub>2</sub>B, and M<sub>3</sub>B (where M is Fe or Fe-Ni and B is S or P). Samples of these sulfide and phosphide phases are often found in meteorites [Britvin *et al.*, 2002; Buseck, 1969; Nazarov *et al.*, 1997, 1998, 2001; Pratesi *et al.*, 2006], which provides additional argument that Fe-Ni-S-P mineral phases are indeed constituents of the cores of planetary bodies. Although reliable information on the high  $P$ - $T$  behavior of sulfide minerals relevant to the planetary cores has been established recently (see Li and Fei [2003] for review), similar information on the analogous phosphides is far from complete.

<sup>1</sup>Center for Advanced Radiation Sources, Argonne National Laboratory, University of Chicago, Argonne, Illinois, USA.

<sup>2</sup>High Pressure Science and Engineering Center, University of Nevada, Las Vegas, Nevada, USA.

<sup>3</sup>Argonne National Laboratory, Argonne, Illinois, USA.

<sup>4</sup>Department of Geosciences, University of Arizona, Tucson, Arizona, USA.

<sup>5</sup>Geophysical Laboratory, Carnegie Institution of Washington, Washington, D. C., USA.

[3] One of the interesting phases in the Fe-P system is di-iron phosphide (Fe<sub>2</sub>P). Fe<sub>2</sub>P occurs in nature in two polymorphic forms, hexagonal barringerite (space group *P*-62m, C22 structure type [Buseck, 1969]) and orthorhombic allabogdanite (space group *Pnma*, C23 structure type [Britvin *et al.*, 2002]). Recently, Dera *et al.* [2008] studied the high-pressure and high-temperature behavior and transformations of synthetic barringerite Fe end-member (Fe<sub>2</sub>P) and found that the ambient, hexagonal phase transforms to the orthorhombic C23-type polymorph upon heating to 1000 K above 8 GPa. The occurrence of the orthorhombic phase in natural meteoritic samples, which has recently been reported in the Onello meteorite [Britvin *et al.*, 2002], provides important clues about the thermodynamic history of the meteorite and the *P*-*T* conditions on the parent body [Dera *et al.*, 2008]. In natural meteoritic barringerite, a fraction of the iron atoms is replaced by nickel and cobalt. The recent experiments [Dera *et al.*, 2008] demonstrate that the C22→C23 transformation is intrinsic to pure Fe<sub>2</sub>P. It has also been suggested that the nickel and/or cobalt present in the structure may have a stabilizing effect on the orthorhombic structure [Britvin *et al.*, 2002].

[4] Understanding the phase equilibria and partitioning of nickel and cobalt between the mantle and outer core is key to reconstructing the core formation mechanism. During the core formation the siderophile Ni and Co are strongly partitioned into the metallic core and become depleted in the mantle [Chabot and Agee, 2002; Chabot *et al.*, 2005]. The partitioning coefficients of Ni and Co determined at ambient pressure suggest that Ni should be an order of magnitude more depleted in the mantle than Co [Walter *et al.*, 2000], whereas the observed depletion is almost equal. In order to understand this discrepancy we need to understand the effects of pressure and temperature [Chabot and Agee, 2002; Chabot *et al.*, 2005], as well as the actual crystallographic and chemical nature of the iron-rich phases (with minor Ni and Co content) present in the core, which may cause the partitioning coefficients to be different from those for pure iron.

[5] At ambient pressure the X-T phase diagram of the Ni-P system [Yupko *et al.*, 1986] is more complicated than that of Fe-P [Zaitsev *et al.*, 1995]. Ambient pressure studies of the phase equilibria in the metal-rich part of the Fe-Ni-P phase diagram [Drabek, 2006; Fruchart *et al.*, 1969] demonstrate complete solid solution in the hexagonal C22 structure at 900°C. To our knowledge, with the exception of Fujii and Okamoto's [1980] study, no other high-pressure studies have been conducted with solid solution (Fe<sub>1-x</sub>Ni<sub>x</sub>)<sub>2</sub>P samples, making understanding of the effects of Ni on the compression behavior of natural barringerite and allabogdanite difficult. Only one high-pressure study on Ni<sub>2</sub>P exists in the literature [Fujii *et al.*, 1981]; the study shows that (1) the compressibility of Ni<sub>2</sub>P is lower than Fe<sub>2</sub>P, (2) the *c/a* ratio in Ni<sub>2</sub>P has an inverse compression behavior compared to Fe<sub>2</sub>P, and (3) up to 10 GPa the volume compression is almost linear. Furthermore, no phase transition was found in Ni<sub>2</sub>P up to 10 GPa on cold compression (ambient temperature). The study of Fujii *et al.* [1981] was constrained to the low-pressure regime and was challenged by significant technical limitations, leading to relatively large uncertainties in the measurements (e.g., the changes in unit cell parameters were refined on the basis of only three diffrac-

tion peaks), and extrapolation of the determined trends to the Earth core conditions would be unreliable.

[6] Motivated to explain the unusual effects observed in Ni<sub>2</sub>P and elucidate the properties of (Fe<sub>1-x</sub>Ni<sub>x</sub>)<sub>2</sub>P solid solution, we performed synchrotron powder X-ray diffraction experiments with synthetic Ni<sub>2</sub>P in a laser-heated diamond anvil cell (DAC) to 50 GPa and 2200 K. Our experiments have been designed to address the following pressing questions: (1) is the ambient, C22 phase stable at high pressure and high temperature; (2) does the C22→C23 phase transition occur in Ni<sub>2</sub>P at higher pressure and/or on heating; (3) what are the EOS parameters of Ni<sub>2</sub>P; (4) is the inverse behavior of the *c/a* ratio real, what is its structural explanation, and how does it affect the possible phase transition; and (5) what are the consequences of incorporating Ni into the Fe<sub>2</sub>P structure in meteoritic samples?

## 2. Experimental Procedure

[7] Commercial synthetic Ni<sub>2</sub>P, purchased from Sigma-Aldrich (98% purity and -100 mesh), was used in the experiments without further purification. Unit cell parameters of the synthetic sample, determined at ambient conditions (*a* = 5.855(2) Å, *c* = 3.823(7) Å), are in good agreement with literature data [Rundqvist, 1962]. No impurity peaks were detected in the X-ray diffraction patterns of the starting sample. Two polycrystalline fragments (hereinafter referred to as S1 and S2) of the synthetic material with approximate size of 20 × 20 × 5 mm<sup>3</sup> were selected under the microscope and mounted in a diamond anvil cell. Diamond anvils with 0.3 mm diameter culets were mounted on cubic boron nitride backing plates. Re metal foil with initial thickness of 0.25 mm, preindented to 0.030 mm, was used as a gasket. A 0.185 mm diameter hole was electrodrilled in the preindented gasket using an electrical discharge machine. Three ruby spheres were mounted in the sample chamber, next to the samples. The DAC was loaded with Ne gas to 25,000 psi (~0.2 GPa) using the Geo-SoilEnviro Consortium for Advanced Radiation Sources (GSECARS)/Consortium for Materials Properties Research in Earth Sciences gas-loading apparatus [Rivers *et al.*, 2008], and pressure was increased to 3.9 GPa inside the gas-loading vessel. After reaching the target pressure inside the gas vessel, the gasket hole diameter decreased to approximately 0.080 mm, but its size and shape did not change significantly upon further compression up to the highest pressure reached. The samples in the DAC at pressure of 12.5 GPa are shown in Figure 1a.

[8] X-ray diffraction data were collected at the insertion device station 13IDD of the GSECARS facility at the Advanced Photon Source, Argonne National Laboratory. The monochromatic incident beam wavelength was 0.3344 Å, and the beam was focused using a pair of Kirkpatrick-Baez mirrors to a focal spot of approximately 0.005 by 0.008 mm. A MAR165 charge-coupled device (CCD) detector, placed approximately 240 mm from the sample, was used to record the diffraction images. The sample was kept still during the exposure, with a typical exposure time of 5 s. The data were processed using FIT2D software [Hammersley, 1998]. The pressure inside the DAC was determined by means of the ruby fluorescence method and calculated using the Mao *et al.* [1986] pressure scale. Integrated diffraction patterns

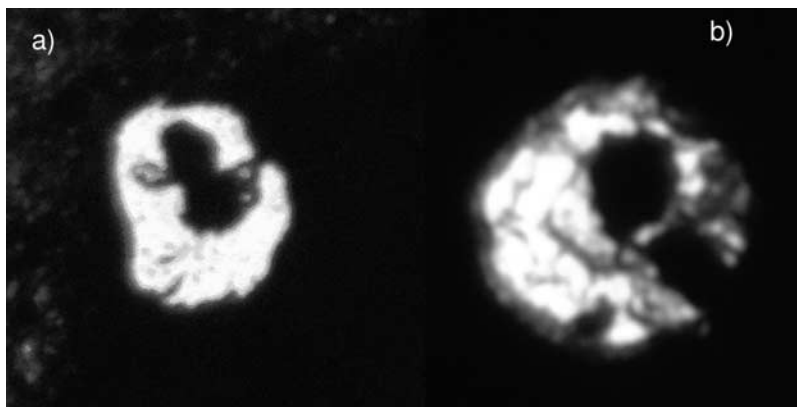


**Figure 1.** Samples used in the two independent high-pressure laser-heating experiments. (a) In the first experiment two polycrystalline aggregates of Ni<sub>2</sub>P are mounted inside a hole drilled in the Re gasket, directly on the surface of the diamond anvil, with Ne pressure medium (shown at 12.5 GPa). (b) In the second experiment the Ni<sub>2</sub>P samples are mounted on top of single-crystal MgO (transparent slabs underneath the black aggregates), which serve as thermal insulator and pressure gauge (shown at 3.6 GPa), also with Ne as pressure medium.

were analyzed with the GSE\_shell software [Dera, 2008], including multiphase Le Bail refinements.

[9] The sample was pressurized in approximately 5 GPa steps. At each pressure step the S2 sample was heated from both sides of the DAC using two diode-pumped fiber lasers, operating at a wavelength of 1.064  $\mu\text{m}$  [Prakapenka *et al.*, 2008]. The thermal emission spectra from the heated spot were measured with a pair of spectrometers with CCD detectors, and the temperature on either side of the heated spot was determined by fitting the blackbody radiation spectrum [Shen *et al.*, 2001]. The maximum temperature reached in the heating experiments was approximately 1800 K at most pressure points.

[10] In order to verify the intriguing observations from the laser heating experiment, which are described in detail in section 3, we performed a second laser-heating experiment with a new sample. This time, in order to optimize the heating efficiency, the polycrystalline Ni<sub>2</sub>P sample was mounted in a DAC on top of a slab of single-crystal MgO, as shown in Figure 1b. The thicknesses of both the MgO crystal and the Ni<sub>2</sub>P aggregate were chosen to be thin enough ( $\sim 0.005$  mm each) to assure that the MgO-Ni<sub>2</sub>P stack did not bridge the two diamond anvils, leaving enough space for the Ne pressure medium. The MgO crystal served both as a thermal insulator and as an additional pressure calibrant. The sample was pressurized to 15 GPa and then heated for approximately 30 min at increasing temperature, ranging from 1300 to 2200 K, with diffraction data collected during the heating, as well as after the temperature quench.

### 3. Results and Discussion

#### 3.1. Incongruent Melting

[11] There was no indication of the C22 $\rightarrow$ C23 transformation in the S2 sample to the highest pressure reached (50 GPa), despite heating after each pressure increase up to and past the ambient melting temperature (melting was indicated by the appearance of diffuse scattering; at ambient pressure the melting temperature of Ni<sub>2</sub>P is 1383 K [Yupko *et al.*, 1986]). Instead, another transformation was detected.

On heating at the second pressure point ( $P = 6.5$  GPa), after significant recrystallization of the sample, in addition to the hexagonal Ni<sub>2</sub>P, a new phase was observed, which was identified as pyrite-type cubic NiP<sub>2</sub> with space group  $Pa\bar{3}$  ( $a = 5.366(3)$   $\text{\AA}$ , C2 structure type), as shown in Figure 2. No traces of this phase were present in the sample prior to the heating. The structures and coordination environments of the metal atoms in the Ni<sub>2</sub>P and NiP<sub>2</sub> structures are quite different, as compared in Figure 3. Cubic NiP<sub>2</sub> was first synthesized by Donohue *et al.* [1968] from a phosphorus-rich mixture of elements corresponding to compositions of NiP<sub>2</sub> and NiP<sub>3</sub> at high pressure and high temperature (6.5 GPa and 1100 $^{\circ}\text{C}$ ). The experiments by Donohue *et al.* [1968] demonstrate that at high pressure the cubic phase of NiP<sub>2</sub> is more stable than the ambient NiP<sub>2</sub> (monoclinic C2/c [Larsson, 1965]). Furthermore, the formation of NiP<sub>2</sub> is favored over a relatively wide range of compositions. Formation of pyrite-type nitrides of noble metals at high pressure and high temperature was recently reported [Crowhurst *et al.*, 2006], demonstrating the high-pressure stability of this cubic structure in a wide range of nitride compositions. In the first experiment, owing to difficulties with maintaining stable heating close to the melting point, it was hard to assess with certainty whether the transformation occurs below or on melting; however, the fact that we see the unambiguous signature of NiP<sub>2</sub> only in diffraction patterns showing significant recrystallization suggests that the two processes (melting and decomposition) are associated.

[12] A chemical reaction transforming Ni<sub>2</sub>P to NiP<sub>2</sub> should result in formation of either elemental nickel or very Ni-rich Ni-P alloy; however, no indication of fcc nickel was observed in our diffraction patterns. There are two possible explanations for this fact: (1) the observed cubic phase could be in the antipyrite structure, preserving Ni<sub>2</sub>P composition, or (2) instead of elemental nickel, an amorphous Ni-P glass was formed. Possibility 1 seems less likely, mainly because of the almost twofold difference in atomic radii between P and Ni, which would cause the antiphase structure to have a significantly different unit cell volume than the cubic NiP<sub>2</sub>. The ambient unit cell volume we observed,

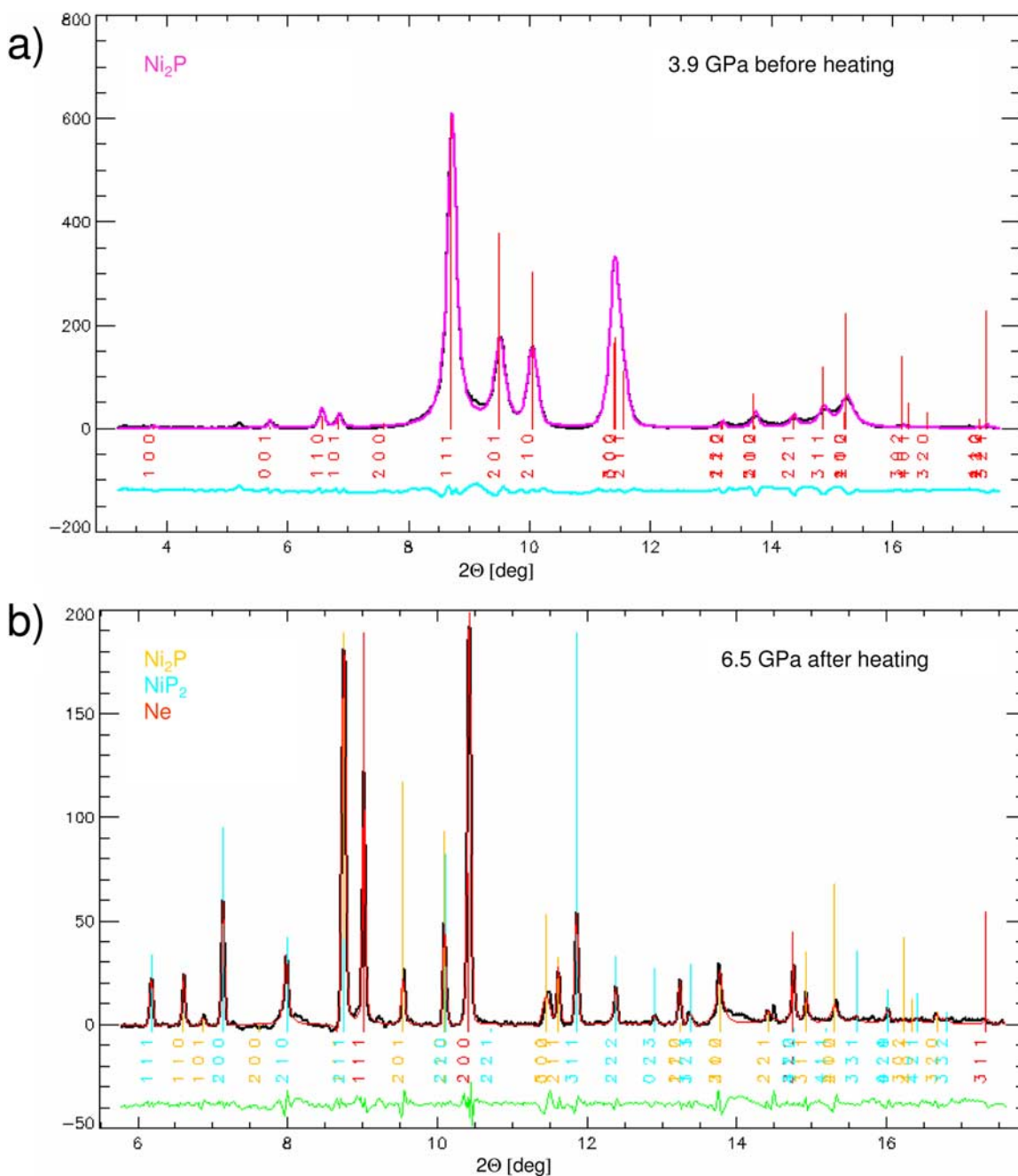


**Figure 2.** Diffraction patterns illustrating the effect of incongruent melting of Ni<sub>2</sub>P. At 3.9 GPa before heating, the starting sample shows no indication of the cubic phase, as shown by the results of Le Bail full pattern refinement (the blue curve shows the difference between the experimental pattern and calculated pattern based on a single phase sample). At 6.5 GPa after laser heating in addition to the original, Ni<sub>2</sub>P phase (yellow), cubic, pyrite-type NiP<sub>2</sub> (blue) is observed. At this pressure, Ne becomes solid and contributes its diffraction lines as well. Because of sample recrystallization, peak intensities cannot be analyzed quantitatively; however, a good qualitative agreement with calculated intensities (vertical bars) is apparent. On melting above 40 GPa, NiP<sub>2</sub> is no longer detectable.

160.0(7) Å<sup>3</sup>, is in good agreement with the volume determined by *Donohue et al.* [1968], 163.7 Å<sup>3</sup>, the small 2% difference suggesting a slight nonstoichiometry. A definite answer to the question of whether the cubic phase observed in our experiments has a pyrite or antipyrite structure would require a single-crystal experiment with a sufficiently large quenched sample.

[13] Ni-rich amorphous alloys in the Ni-P system are well known and widely used in technological applications [*Tanaka et al.*, 2007]. While Ni-P metallic glasses form with excess free volume and are expected to crystallize by structural relaxation at high temperature [*Greer*, 1984], pressure may have a stabilizing effect on the glassy state. Nonequilibrium glass formation on rapid quench from melt

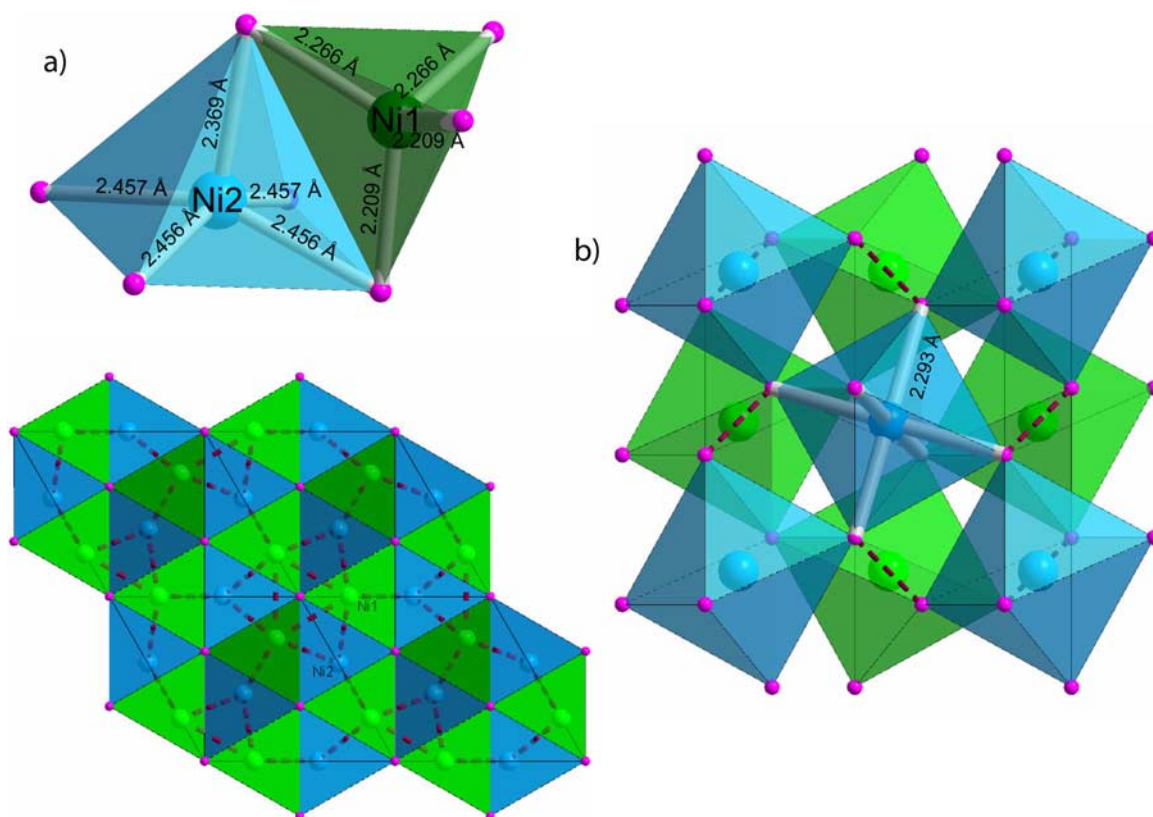


**Figure 3.** Comparison of the crystal structures of (a) hexagonal Ni<sub>2</sub>P and (b) cubic NiP<sub>2</sub>. Dashed lines indicate short Ni-Ni contacts in Ni<sub>2</sub>P and P-P contacts in NiP<sub>2</sub>.

is quite common in petrology. Earlier high-pressure studies with Ni-P amorphous alloys demonstrate that the crystallization temperature increases on compression [Imura *et al.*, 1988; Linden *et al.*, 1987]. Several examples of stable glasses that form at high pressure and high temperature exist in the literature, including the recent discovery of CO<sub>2</sub> “carbonia” glass [Santoro *et al.*, 2006]. Furthermore, Li *et al.* [2007] recently demonstrated that Ni-P amorphous alloys can be stable to significant pressures (at least 30 GPa). It is likely that the broad, amorphous features from very minute amounts of Ni-P glass formed in our experiments were not detectable because of the high-scattering background in the DAC.

[14] Yupko *et al.* [1986] reported that at ambient pressure Ni<sub>2</sub>P melts congruently; therefore, our observation of cubic NiP<sub>2</sub> formation suggests two important new facts about the phase equilibria in the Ni-P system: (1) the cubic NiP<sub>2</sub> phase can be formed at high pressure even with significant excess of Ni, and (2) the character of melting of Ni<sub>2</sub>P changes from congruent to incongruent at high pressure.

[15] Melting experiments at high pressure are typically performed with a solid pressure medium (usually NaCl), which assures good thermal insulation of the sample from diamond anvils. Use of Ne in our experiments provided excellent hydrostaticity but at the same time made it difficult to maintain uniform and stable heating close to the melting point. Ne, which has a much lower melting temperature than Ni<sub>2</sub>P, becomes liquid in the vicinity of the hot spot and allows the Ni<sub>2</sub>P crystallites to move around by convection. While we were able to observe a decrease in the diffraction signal

from the sample and growth of the amorphous scattering signal, we were never able to sustain a completely molten sample for long enough to observe a completely amorphous scattering pattern. This made it impossible to unambiguously assess the melting curve at high pressure. Despite efforts at fully converting the sample to NiP<sub>2</sub>, we were also not able to achieve a complete transformation, as the diffraction patterns always revealed a mixture of the two previously identified crystalline phases. The only diffraction pattern showing almost exclusively NiP<sub>2</sub> and Ne crystalline contributions was collected at 12.2 GPa during heating at 1400 K. Because of the recrystallization of the sample upon heating and severe preferred orientation, it was not possible to use the peak intensity information for structural refinement or phase fraction analysis. Despite the chemical reaction, the unit cell parameters of the Ni<sub>2</sub>P phase from the heated spot remained in good agreement with the unit cell parameters of the unheated sample, suggesting that the stoichiometry of the remaining Ni<sub>2</sub>P does not change noticeably. Presence of NiP<sub>2</sub> was clearly detectable on heating up to about 40 GPa; however, on heating at higher pressures the content of the new phase decreased significantly, suggesting that the incongruent character of the Ni<sub>2</sub>P melting is constrained to only a range of pressures and becomes congruent again above 40 GPa. Interestingly, similar behavior has been recently observed in the closely related Fe<sub>3</sub>C system (V. B. Prakapenka, unpublished data, 2008).

[16] In order to confirm the interesting observation of the pyrite-type NiP<sub>2</sub> phase formation we repeated the heating experiment with a new sample, this time mounted on top of

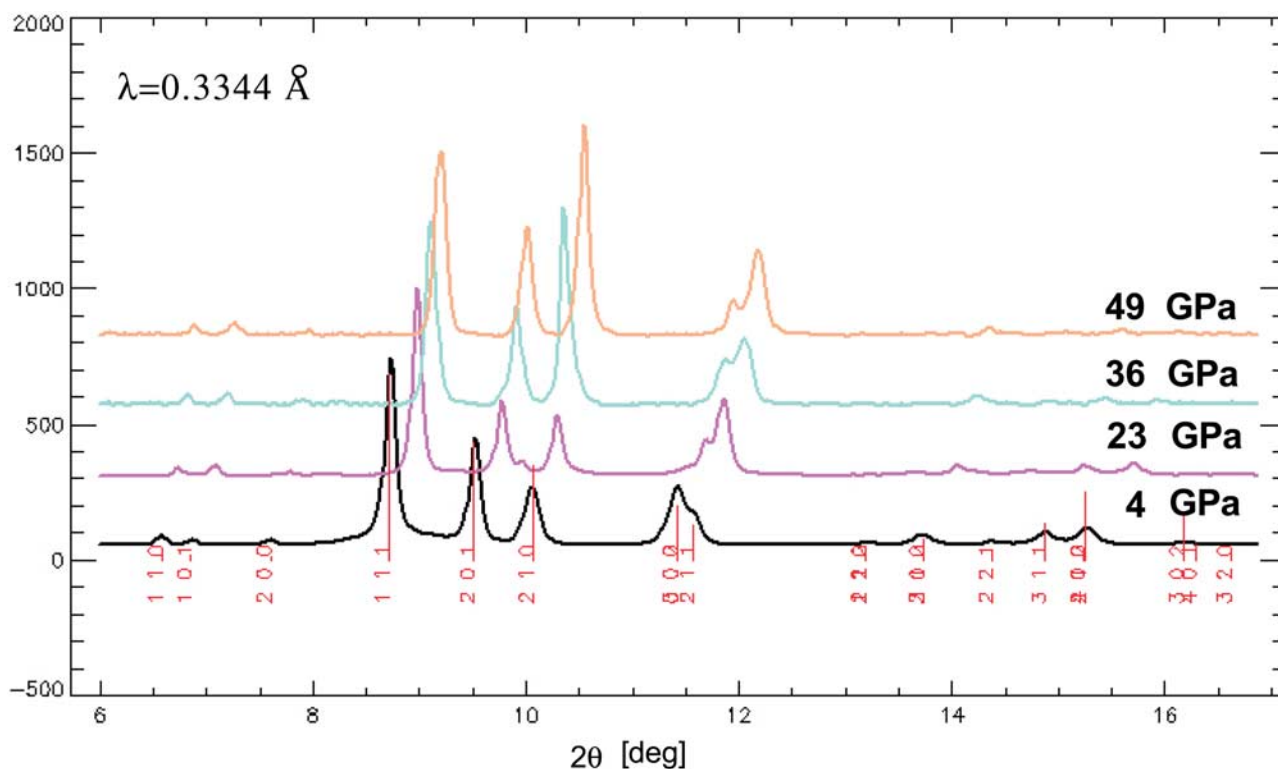


**Figure 4.** Evolution of the diffraction pattern of the unheated, S1 sample of Ni<sub>2</sub>P on compression to 50 GPa.

a single crystal of MgO to assure good thermal insulation from the diamond anvils during heating. Again, prior to heating, the starting sample showed no signs of the cubic NiP<sub>2</sub>. Heating was performed at 15 GPa between temperatures of 1300 and 2200 K. This time the heating was much more efficient and uniform, and it was possible to keep the sample at high temperature for an extended time (up to 30 min). A clear signature of NiP<sub>2</sub> formation was detected above 1300 K and on temperature quench. Despite the improved heating (thanks to the MgO insulation), we were again not able to completely convert the sample to NiP<sub>2</sub>. This observation further supports the hypothesis that the observed phenomenon involves a chemical reaction rather than a phase transition, since in the latter case with sufficient heating the thermodynamically stable phase should be the only product. The chemical reaction occurring between the high-temperature phase and the melt, on the other hand, could be significantly affected by fractional crystallization (precipitation of NiP<sub>2</sub> and its removal from the hot spot by convection), which would locally change the composition in the system and could explain the incomplete transformation.

### 3.2. Compression Behavior and Equation of State

[17] In contrast to the heated S2 sample, the diffraction patterns of the unheated S1 Ni<sub>2</sub>P showed only continuous changes throughout the whole studied pressure range (Figure 4). The compression data obtained from S1 confirm the observation of *Fujiwara et al.* [1981] that unlike Fe<sub>2</sub>P, Ni<sub>2</sub>P exhibits a decrease of *c/a* at high pressure.

[18] The ambient temperature bulk modulus  $K_0$  and its pressure derivative  $K'$  have been calculated by fitting the third-order Birch-Murnaghan equation of state, with the

ambient volume fixed ( $V_0 = 100.54 \text{ \AA}^3$ ) to the experimental unit cell data. The final values of the optimized parameters are presented in Table 1 and are compared with the bulk moduli of Fe<sub>2</sub>P, as well as elemental Fe and Ni. Figure 5 presents a comparison of our compression data with those of *Fujiwara et al.* [1981]. The two experiments show reasonable agreement in the pressure range up to 10 GPa; however, extrapolation of the linear trends of *Fujiwara et al.* [1981] to 50 GPa leads to overestimation of the unit cell volume by more than 10%, which is significant but typical with extrapolation of lower-pressure data.

[19] With a bulk modulus of  $K_0 = 201(8)$  GPa and its pressure derivative  $K' = 4.2(6)$ , Ni<sub>2</sub>P is significantly less compressible (by about 10%) than Fe<sub>2</sub>P ( $K_0 = 175(8)$ ,  $K' = 4$  [*Dera et al.*, 2008]). When fitted over a sufficiently wide pressure range, the optimized pressure derivative of the bulk modulus  $K'$  has a very reasonable value, and the compression does not exhibit quasi-linear behavior as previously observed over a limited pressure range [*Fujiwara et al.*, 1981]. Pure elemental nickel in the fcc phase is less compressible than hcp elemental iron ( $K_0 = 165$  GPa for Fe [*Dewaele et al.*, 2006], and  $K_0 = 180$  GPa for Ni [*Chen et al.*, 2000]), suggesting that replacement of Fe by Ni in (Fe<sub>1-x</sub>Ni<sub>x</sub>)<sub>2</sub>P should increase the bulk modulus only slightly. The observed magnitude of the difference in compressibility between Fe<sub>2</sub>P and Ni<sub>2</sub>P is larger than expected, which is not entirely surprising considering the significant departures from the Vegard rule in (Fe<sub>1-x</sub>Ni<sub>x</sub>)<sub>2</sub>P reported by *Fruchart et al.* [1969].

[20] The main difference between Fe<sub>2</sub>P and Ni<sub>2</sub>P at ambient pressure is their magnetic order [*Ishida et al.*, 1987]. Fe<sub>2</sub>P is ferromagnetic with a Curie temperature of 209 K, whereas Ni<sub>2</sub>P is paramagnetic [*Ishida et al.*, 1987].

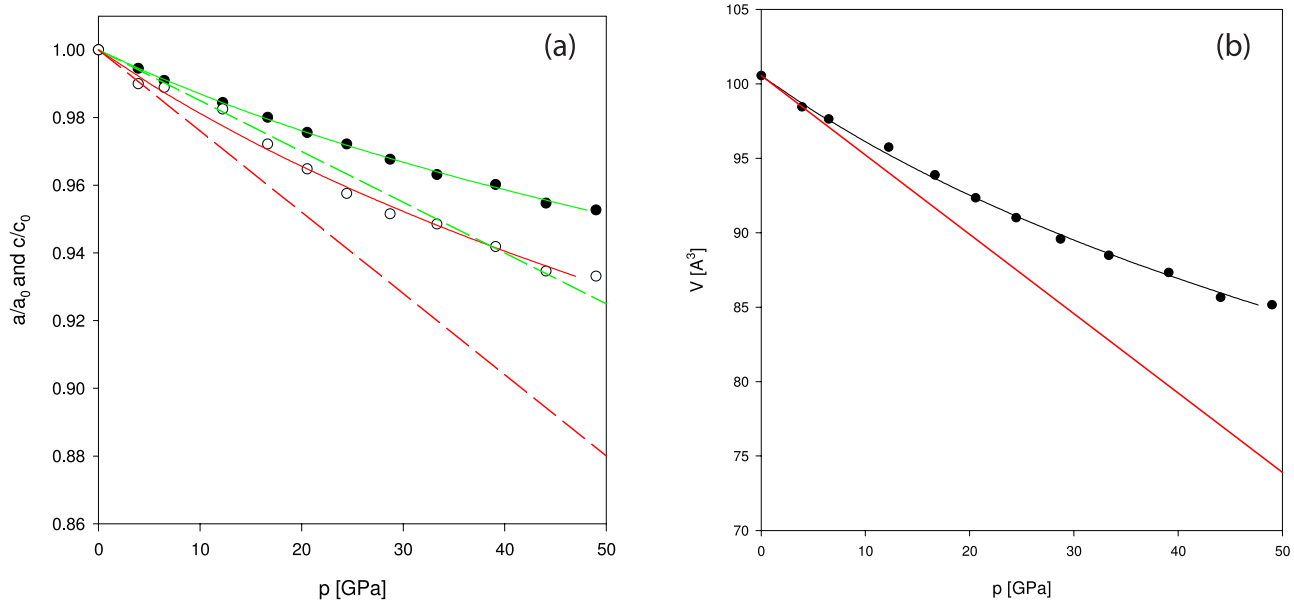


**Figure 5.** Evolution of (a) unit cell parameters and (b) unit cell volume as a function of pressure. Solid line shows third-order Birch-Murnaghan EOS fit to the experimental data. Straight lines show quasi-linear trends reported by *Fujiwara et al.* [1981].

In Fe<sub>2</sub>P there is a clear correlation between the  $c/a$  ratio and the ferromagnetic interactions. *Fujiwara et al.* [1982] demonstrated that uniaxial stress applied to a single crystal of Fe<sub>2</sub>P along the  $c$  axis (i.e., decreasing the  $c/a$  ratio) increases  $T_c$  and destabilizes the ferromagnetic state, whereas similar stress applied perpendicular to the  $c$  direction has an opposite effect and decreases  $T_c$ , stabilizing the ferromagnetic state. On hydrostatic compression,  $T_c$  decreases (as  $c/a$  increases) and vanishes at 1.3 GPa [*Abliz et al.*, 2006].

[21] In crystal chemistry and mineral physics, high-pressure compression trends are often compared with chemical compression trends (chemical substitution without change of the crystal structure) [see, e.g., *Hazen and Finger*, 1982]. Several studies have been reported on the solid solution effects in Fe<sub>2</sub>P, involving replacement of part of the P atoms by Si, As, and B, which are worth comparing with the high-pressure compression behavior of Ni<sub>2</sub>P and Fe<sub>2</sub>P. On the one hand, both Si [*Jernberg et al.*, 1984] and As [*Catalano et al.*, 1973] substitutions expand the unit cell volume of Fe<sub>2</sub>P and cause  $c/a$  to decrease. The B substitution, on the other hand, causes volume contraction and decreases the  $c/a$  ratio, exactly like high-pressure compression

[*Chandra et al.*, 1980]. All of the substitutions increase the critical temperature, in accordance with their  $c/a$  effect. Furthermore, above a certain critical concentration, increasing the Si and As component causes the orthorhombic C23-type structure to become stable at ambient conditions, whereas boron does not show a similar effect. *Fruchart et al.* [1969] reported solid solution studies involving metal site substitutions with Fe, Ni, Co, Mn, and Cr phosphides. Ni-Fe-P is the only ternary system which does not exhibit the orthorhombic phase at ambient pressure. In the other systems, increasing Mn, Co, and Cr content causes a  $c/a$  ratio increase and produces a C22→C23 transition at some critical concentration; however, (Fe<sub>1-x</sub>Mn<sub>x</sub>)<sub>2</sub>P and (Ni<sub>1-x</sub>Mn<sub>x</sub>)<sub>2</sub>P show a more complicated behavior, with the orthorhombic phase stable only in an intermediate range of concentrations. In conclusion, in Fe<sub>2</sub>P the interaction between the ferromagnetically ordered Fe atoms along the  $c$  direction makes that direction less compressible than the  $a$  direction, whereas in paramagnetically disordered Ni<sub>2</sub>P, lack of a magnetic interaction makes  $c$  more compressible than  $a$ .

[22] Since the cubic NiP<sub>2</sub> phase was observed over a wide pressure range, we determined the pressure evolution of its

**Table 1.** Equation of State Parameters for Possible Light Element Alloys in the Earth Core

Compound	Structure Type	$K_0$	$K'$	$V_0$	Reference
NiP <sub>2</sub>	C2	184(4)	4.2(2)	160.0(1)	this paper
FeS <sub>2</sub>	C2	133.5(5)	5.7(6)	159.9(fixed)	<i>Merkel et al.</i> [2002]
Ni <sub>2</sub> P	C22	201(8)	4.2(6)	100.54(fixed)	this paper
Fe <sub>2</sub> P	C22	175(8)	4.0(fixed)	103.16(1)	<i>Dera et al.</i> [2008]
Fe <sub>2</sub> P	C23	177(3)	4.0(fixed)	137.95(3)	<i>Dera et al.</i> [2008]
Fe <sub>3</sub> P	DOe	159(1)	4.0(fixed)	369.3(fixed)	<i>Scott et al.</i> [2007]
Fe <sub>3</sub> S	DOe	156(7)	3.8(3)	377.01	<i>Seagle et al.</i> [2006]
Fe <sub>3</sub> C	cementite	175(4)	5.2(3)	155.3(1)	<i>Scott et al.</i> [2001]
Ni <sub>2</sub> Si	C23	167(5)	4.5(5)	131.05(fixed)	<i>Errandonea et al.</i> [2008]
Fe	hcp	163(8)	5.3(2)	11.21(5)	<i>Dewaele et al.</i> [2006]
Ni	fcc	185.4(10)	4.0(fixed)	43.7(fixed)	<i>Chen et al.</i> [2000]

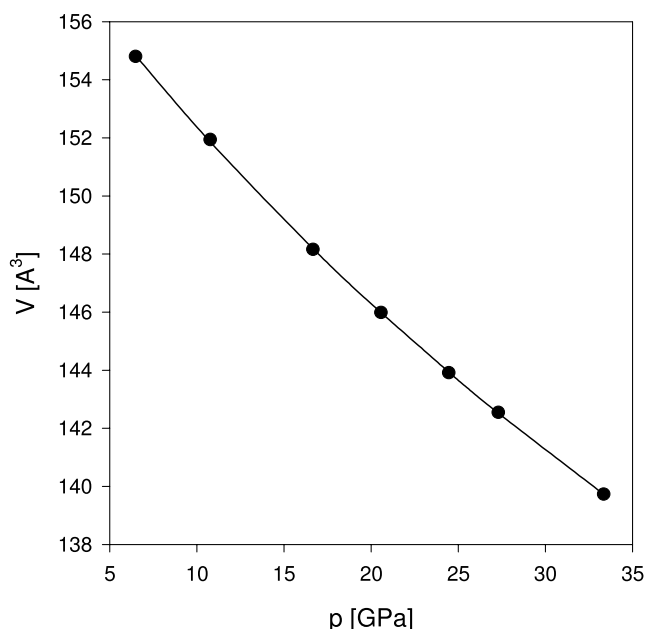


**Figure 6.** Evolution of the unit cell volume of the cubic FeP<sub>2</sub> phase as a function of pressure. Solid line shows third-order Birch-Murnaghan EOS fit to the experimental data.

unit cell volume and performed a third-order Birch-Murnaghan EOS fit (Figure 6). The bulk modulus of the cubic NiP<sub>2</sub>  $K_0 = 189(9)$  GPa and  $K' = 4.2(2)$  ( $K_0 = 172(1)$  GPa with  $K'$  fixed at 4.0) is noticeably higher than the bulk modulus of isostructural pyrite, FeS<sub>2</sub> ( $K_0 = 133.5$  GPa,  $K' = 5.73$  [Kleppe and Jephcoat, 2004]), and the refined ambient volume  $V_0 = 160.0(7)$  Å<sup>3</sup> is in reasonable agreement with  $V_0 = 163.7$  Å<sup>3</sup> reported by Donohue *et al.* [1968].

### 3.3. C22→C23 Transition and Effect of Ni Substitution in Meteoritic Allabogdanite

[23] The opposite trends of the  $c/a$  ratio with pressure in Ni<sub>2</sub>P and Fe<sub>2</sub>P suggest that the trend followed by high-pressure compression of Ni<sub>2</sub>P does not lead into the C23 structure stability. While no experimental data exist on solid solutions of Ni<sub>2</sub>P involving nonmetal substituents, it is possible that such chemical substitution could lead to stabilization of the C23 structure. Indeed, an orthorhombic C23-type polymorph has been observed for Ni<sub>2</sub>Si at ambient pressure [Toman, 1952]. The natural occurrence of allabogdanite with significant Ni content proves that a substitution in the metal sites of the Ni<sub>2</sub>P structure can also stabilize the orthorhombic phase; however, the trends determined for the pure Ni<sub>2</sub>P system make it hard to believe that Ni is the stabilizing agent. Fujii and Okamoto [1980] demonstrated that the introduction of Ni into Fe<sub>2</sub>P suppresses the stabilizing effect of pressure on the ferromagnetic order (decrease of  $T_c$  on compression), and the effect vanishes at Ni concentrations exceeding 30 at. %. The Fe component and the associated magnetic ordering seem essential for the stabilization of Ni-containing allabogdanite. In addition to Ni, meteoritic allabogdanite was found to contain 3% Co [Britvin *et al.*, 2002]. In Co<sub>2</sub>P, the orthorhombic C23 structure is stable (or at least metastable) at ambient conditions [Ellner and Mittemeijer, 2001], suggesting that unlike Ni, the

presence of Co should have a strong stabilizing effect on allabogdanite. The recent solid solution study of Drabek [2006], however, demonstrates that the amount of Co in their particular meteoritic sample is insufficient to stabilize the orthorhombic structure at ambient pressure. As a consequence, the barringerite-to-allabogdanite transition must have originated at high pressure and high temperature, while the Co content probably decreased the pressure threshold of the transformation.

## 4. Conclusions

[24] We found the high-pressure behavior of the barringerite Ni end-member to be quite different from that of the Fe end-member. Ni<sub>2</sub>P is paramagnetic and lacks the ferromagnetic interaction along the hexagonal 001 direction. It shows a decrease of the  $c/a$  ratio at high pressure, in contrast to the  $c/a$  increase observed in Fe<sub>2</sub>P. At high temperatures and at pressures between 6.5 and 40 GPa, Ni<sub>2</sub>P melts incongruently, apparently decomposing to a pyrite-type high-pressure phase of NiP<sub>2</sub> and amorphous Ni-P alloy, but the melting becomes congruent again above 40 GPa. NiP<sub>2</sub> is noticeably less compressible than either pure hcp iron or any previously studied iron phosphide phase. The C22→C23 phase transition does not occur in Ni<sub>2</sub>P up to at least 50 GPa. As a consequence, the Ni content in meteoritic barringerite is unlikely to have a stabilizing effect on the orthorhombic allabogdanite structure and at significant concentrations may, in fact, increase the threshold pressure at which such a transformation is favored.

[25] In the Fe-S-P system, pressure was demonstrated to have a rather minor effect on the X-T phase diagram [Stewart and Schmidt, 2007], whereas the occurrence of the NiP<sub>2</sub> phase across a wide range of compositions in the Ni-P phase diagram at high pressure suggests that the pressure effect in the Ni-P-S system is rather dramatic. FeP<sub>2</sub> is not known to assume the pyrite-type structure; instead, it crystallizes in the orthorhombic marcasite structure [Holseth and Kjekshus, 1968]. Furthermore, heating experiments with Fe<sub>2</sub>P reveal no indications of chemical reactions [Dera *et al.*, 2008]. As a consequence, contrary to the current beliefs, the Ni content in planetary cores may significantly affect the phase equilibria. While physical and chemical properties of NiP<sub>2</sub> and Ni<sub>2</sub>P have not yet been examined in detail, the crystal structures of NiP<sub>2</sub> and Ni<sub>2</sub>P are quite different, with different coordination environments of the metal atoms, and are very likely to produce notable differences in electrical and thermal conductivity as well as diffusion and partitioning properties with regard to other elements relevant to the core-mantle boundaries (CMB) of planetary bodies. Chen *et al.* [2008] recently demonstrated for the Fe-FeS system that pressure-controlled chemical reactions leading to stability of different stoichiometric compounds at varied thermodynamic conditions can affect the shape of liquidus curves, with potentially significant consequences for convection and precipitation processes at CMBs. The estimated  $P$ - $T$  conditions of the Earth's CMB fall outside of the incongruent melting pressure range of Ni<sub>2</sub>P, but the conditions of the CMB on Mars and Mercury are well within that range. It remains to be verified experimentally whether the high-pressure phase diagram of Ni-S resembles that of Ni-P, but with the significant Ni and S

content of the Martian and Mercurian cores and the wide compositional range of stability of NiP<sub>2</sub> (and perhaps NiS<sub>2</sub>) it can be expected that Ni(S,P)<sub>2</sub> may be an important constituent of the cores of these planets.

[26] **Acknowledgments.** We would like to thank S. D. Jacobsen for kindly providing the polished MgO crystals used in one of the laser-heating experiments. This project was supported by a grant from the MRI Program, Division of Materials Research, National Science Foundation (NSF-DMR-0521179). X-ray data were collected at GSECARS (Sector 13), Advanced Photon Source (APS), Argonne National Laboratory. GSECARS is supported by the National Science Foundation—Earth Sciences (EAR-0622171) and Department of Energy—Geosciences (DE-FG02-94ER14466). Use of the Advanced Photon Source was supported by the U.S. Department of Energy, Office of Science, Office of Basic Energy Sciences, under contract DE-AC02-06CH11357.

## References

- Abliz, M., Y. Uwatoko, T. Ohki, and H. Fuji (2006), New pressure-induced phase transitions in Fe<sub>2</sub>P, *J. Phys. Soc. Jpn.*, *75*, 123706, doi:10.1143/JPSJ.75.123706.
- Allegre, C. J., J. P. Poirier, E. Humles, and A. W. Hofmann (1995), The chemical composition of the Earth, *Earth Planet. Sci. Lett.*, *134*, 515–526, doi:10.1016/0012-821X(95)00123-T.
- Birch, F. (1952), Elasticity and constitution of the Earth's interior, *J. Geophys. Res.*, *57*, 227–286, doi:10.1029/JZ057i002p00227.
- Britvin, S. N., N. S. Rudashevsky, S. V. Krivovichev, P. C. Burns, and Y. S. Polekhovsky (2002), Allabogdanite (Fe,Ni)<sub>2</sub>P, a new mineral from the Onello meteorite: The occurrence and crystal structure, *Am. Mineral.*, *87*, 1245–1249.
- Buseck, P. (1969), Phosphide from meteorites: Barringerite, a new iron-nickel mineral, *Science*, *165*, 169–171, doi:10.1126/science.165.3889.169.
- Catalano, A., R. J. Amott, and A. Wold (1973), Magnetic and crystallographic properties of the system Fe<sub>2</sub>P<sub>1-x</sub>As<sub>x</sub>, *J. Solid State Chem.*, *7*, 262–268, doi:10.1016/0022-4596(73)90132-1.
- Chabot, N. L., and C. B. Agee (2002), The behavior of nickel and cobalt during core formation, *Lunar Planet. Sci.*, XXXIII, Abstract 1009.
- Chabot, N. L., D. S. Draper, and C. B. Agee (2005), Conditions of core formation in the Earth: Constraints from nickel and cobalt partitioning, *Geochim. Cosmochim. Acta*, *69*, 2141–2151, doi:10.1016/j.gca.2004.10.019.
- Chandra, R., S. Bjarman, T. Ericsson, L. Häggström, C. Wilkinson, and R. Wäppling (1980), A Mössbauer and X-ray study of Fe<sub>2</sub>P<sub>1-x</sub>B<sub>x</sub> compounds ( $x < 0.15$ ), *J. Solid State Chem.*, *34*, 389–396, doi:10.1016/0022-4596(80)90440-5.
- Chen, B., D. Penwell, and M. B. Kruger (2000), The compressibility of nanocrystalline nickel, *Solid State Commun.*, *115*, 191–194, doi:10.1016/S0038-1098(00)00160-5.
- Chen, B., J. Li, and S. A. Hauck (2008), Non-ideal liquidus curve in the Fe-S system and Mercury's snowing core, *Geophys. Res. Lett.*, *35*, L07201, doi:10.1029/2008GL033111.
- Crowhurst, J. C., A. F. Goncharov, B. Sadigh, C. L. Evans, P. G. Morrall, J. L. Ferreira, and A. J. Nelson (2006), Synthesis and characterization of the nitrides of platinum and iridium, *Science*, *311*, 1275–1278, doi:10.1126/science.1121813.
- Dera, P. (2008), GSE\_shell data analysis program for monochromatic powder diffraction with area detector, GeoSoilEnviro Consortium for Adv. Radiat. Sources, Chicago, Ill.
- Dera, P., B. Lavina, L. A. Borkowski, V. B. Prakapenka, S. R. Sutton, M. L. Rivers, R. T. Downs, N. Z. Boctor, and C. T. Prewitt (2008), High-pressure polymorphism of Fe<sub>2</sub>P and its implications for meteorites and Earth's core, *Geophys. Res. Lett.*, *35*, L10301, doi:10.1029/2008GL033867.
- Dewaele, A., P. Loubeyre, F. Occeli, M. Mezouar, P. I. Dogokupets, and M. Torrent (2006), Quasihydrostatic equation of state of iron above 2 Mbar, *Phys. Rev. Lett.*, *97*, 215504, doi:10.1103/PhysRevLett.97.215504.
- Donohue, P. C., T. A. Bither, and H. S. Young (1968), High-pressure synthesis of pyrite-type nickel diphosphide and nickel diarsenide, *Inorg. Chem.*, *7*, 998–1001, doi:10.1021/ic50063a031.
- Drabek, M. (2006), Phosphide solid-solutions within the metal-rich portion of the quaternary system Co-Fe-Ni-P at 800°C, and mineralogical implications, *Can. Mineral.*, *44*, 399–408, doi:10.2113/gscanmin.44.2.399.
- Ellner, M., and E. J. Mittemeijer (2001), The reconstructive phase transformation  $\beta$ -Co<sub>2</sub>P $\rightarrow$  $\alpha$ -Co<sub>2</sub>P and the structure of the high-temperature phosphide  $\beta$ -Co<sub>2</sub>P, *J. Inorg. Gen. Chem.*, *627*, 2257–2260, doi:10.1002/1521-3749(200109)627:9<2257::AID-ZAAC2257>3.0.CO;2-W.
- Errandonea, D., D. Santamaria-Perez, A. Vegas, J. Nuss, M. Jansen, P. Rodriguez-Hernandez, and A. Munoz (2008), Structural stability of Fe<sub>3</sub>Si<sub>3</sub> and Ni<sub>2</sub>Si studied by high-pressure X-ray diffraction and ab initio total-energy calculations, *Phys. Rev. B*, *77*, 094113, doi:10.1103/PhysRevB.77.094113.
- Fruchart, R., A. Roger, and J. P. Senatur (1969), Crystallographic and magnetic properties of solid solutions of the phosphides M<sub>2</sub>P, M = Cr, Fe, Co, and Ni, *J. Appl. Phys.*, *40*, 1250–1257, doi:10.1063/1.1657617.
- Fujii, H., and T. Okamoto (1980), Effect of pressure on the Curie temperatures of the system (Fe<sub>1-x</sub>Ni<sub>x</sub>)<sub>2</sub>P, *J. Phys. Soc. Jpn.*, *49*, 419–420, doi:10.1143/JPSJ.49.419.
- Fujiwara, H., M. Nomura, H. Kadomatsu, N. Nakagiri, T. Nishizaka, Y. Yamamoto, H. Fujii, and T. Okamoto (1981), Anisotropic lattice compression in Fe<sub>2</sub>P, *J. Phys. Soc. Jpn.*, *50*, 3533–3534, doi:10.1143/JPSJ.50.3533.
- Fujiwara, H., H. Kadomatsu, and K. Tohma (1982), Effect of uniaxial stress on the Curie temperature in Fe<sub>2</sub>P, *J. Phys. Soc. Jpn.*, *51*, 1401–1405, doi:10.1143/JPSJ.51.1401.
- Greer, A. L. (1984), Atomic transport and structural relaxation in metallic glasses, *J. Non Cryst. Solids*, *61–62*, 737–748, doi:10.1016/0022-3093(84)90633-1.
- Hammersley, A. (1998), *FIT2D V10.3 Reference Manual V4.0*, Eur. Synchrotron Radiat. Facil., Grenoble, France.
- Harder, H., and G. Schubert (2001), Sulfur in Mercury's core?, *Icarus*, *151*, 118–122, doi:10.1006/icar.2001.6586.
- Hazen, R. M., and L. W. Finger (1982), *Comparative Crystal Chemistry: Temperature, Pressure, Composition and the Variation of Crystal Structure*, John Wiley, London.
- Holsteth, H., and A. Kjekshus (1968), Compounds with the marcasite type crystal structure. II. On the crystal structures of the binary pnictides, *Acta Chem. Scand.*, *22*, 3284–3292, doi:10.3891/acta.chem.scand.22-3284.
- Imura, T., M. Suwa, and K. Fuji (1988), Effects of ultrahigh pressure on the crystallization temperature of Ni<sub>80</sub>P<sub>20</sub> amorphous alloys, *Mater. Sci. Eng.*, *97*, 247–251, doi:10.1016/0025-5416(88)90051-1.
- Ishida, S., S. Asano, and I. Ishida (1987), Electronic structures and magnetic properties of T<sub>2</sub>P (T = Mn, Fe, Ni), *J. Phys. F Metal Phys.*, *17*, 475–482, doi:10.1088/0305-4608/17/2/016.
- Jernberg, P., A. A. Yousif, L. Häggström, and Y. Andersson (1984), A Mössbauer study of Fe<sub>2</sub>P<sub>1-x</sub>Si<sub>x</sub> ( $x < 0.35$ ), *J. Solid State Chem.*, *53*, 313–322, doi:10.1016/0022-4596(84)90108-7.
- Kleppe, A. K., and A. P. Jephcoat (2004), High-pressure Raman spectroscopic studies of FeS<sub>2</sub> pyrite, *Mineral. Mag.*, *68*, 433–441, doi:10.1180/0026461046830196.
- Larsson, E. (1965), An X-ray investigation of the Ni-P system and the crystal structures of NiP and NiP<sub>2</sub>, *Ark. Kemi*, *23*, 335–365.
- Li, J., and Y. Fei (2003), Experimental constraints on core composition, in *Treatise on Geochemistry*, vol. 2, *The Mantle and Core*, edited by R. W. Carlson, pp. 521–546, Elsevier Sci., Oxford, U. K.
- Li, G., Y. P. Gao, Y. N. Sun, M. Z. Ma, J. Liu, and R. P. Liu (2007), Compression behavior and equation of state of Ni<sub>7</sub>P<sub>23</sub> amorphous alloy, *Chin. Sci. Bull.*, *52*, 440–443, doi:10.1007/s11434-007-0067-6.
- Linden, P., P. Lamparter, and S. Steeb (1987), Crystallization and relaxation of amorphous Mg-Zn, Cu-Ti, and Ni-P alloys under high hydrostatic pressure, *Phys. Status Solidi A*, *104*, 357–368, doi:10.1002/pssa.2211040126.
- Mao, H. K., J. Xu, and P. M. Bell (1986), Calibration of the ruby pressure gauge to 800 kbar under quasi-hydrostatic conditions, *J. Geophys. Res.*, *91*, 4673–4676, doi:10.1029/JB091iB05p04673.
- McDonough, W. F. (2003), Compositional model for the Earth's core, in *Treatise on Geochemistry*, vol. 2, *The Mantle and Core*, edited by R. W. Carlson, pp. 547–568, Elsevier Sci., Oxford, U. K.
- McDonough, W. F., and S. S. Sun (1995), The composition of the Earth, *Chem. Geol.*, *120*, 223–253, doi:10.1016/0009-2541(94)00140-4.
- Merkel, S., A. P. Jephcoat, J. Shu, H. K. Mao, P. Gillet, and R. J. Hemley (2002), Equation of state, elasticity, and shear strength of pyrite under high pressure, *Phys. Chem. Miner.*, *29*, 1–9, doi:10.1007/s002690100207.
- Nazarov, M. A., F. Brandstätter, and G. Kurat (1997), Comparative chemistry of P-rich opaque phases in CM chondrites, *Lunar Planet. Sci.*, XXVIII, Abstract 1466.
- Nazarov, M. A., F. Brandstätter, G. Kurat, and T. Ntaflou (1998), Chemistry of P-rich sulfides in Murchinson, cold Bokkeld and Nagoya CM chondrites, *Lunar Planet. Sci.*, XXXI, Abstract 1466.
- Nazarov, M. A., G. Kurat, and F. Brandstätter (2001), Phosphorian sulfides from the ALH 84029, ALH 85013, and Y 82042 CM carbonaceous chondrites, *Lunar Planet. Sci.*, XXXII, Abstract 1769.
- Prakapenka, V. B., A. Kubo, A. Kuznetsov, A. Laskin, O. Shkurikhin, P. Dera, M. L. Rivers, and S. R. Sutton (2008), Advanced flat top laser heating system for high pressure research at GSECARS: Application to the melting behavior of germanium, *High Pressure Res.*, *28*, 225–236, doi:10.1080/08957950802050718.
- Pratesi, G., L. Bindi, and V. Moggi-Cecchi (2006), Icosahedral coordination of phosphorus in the crystal structure of mellinite, a new phosphide

- mineral from the Northwest Africa 1054 acapulcoite, *Am. Mineral.*, *91*, 451–454, doi:10.2138/am.2006.2095.
- Rivers, M. L., V. B. Prakapenka, A. Kubo, C. Pullins, C. M. Hall, and S. D. Jacobsen (2008), The COMPRES/GSECARS gas loading system for diamond anvil cells at the Advanced Photon Source, *High Pressure Res.*, *28*, 273–292, doi:10.1080/08957950802333593.
- Rundqvist, S. (1962), X-ray investigations of Mn<sub>3</sub>P, Mn<sub>2</sub>P, and Ni<sub>2</sub>P, *Acta Chem. Scand.*, *16*, 992–998, doi:10.3891/acta.chem.scand.16-0992.
- Santoro, M., F. A. Gorelli, R. Bini, G. Ruocco, S. Scandolo, and W. A. Crichton (2006), Amorphous silica-like carbon dioxide, *Nature*, *441*, 857–860, doi:10.1038/nature04879.
- Scott, H. P., Q. Williams, and E. Knittle (2001), Stability and equation of state of Fe<sub>3</sub>C to 73 GPa: Implications for carbon in the Earth's core, *Geophys. Res. Lett.*, *28*, 1875–1878, doi:10.1029/2000GL012606.
- Scott, H. P., S. Huggins, M. R. Frank, S. J. Maglio, C. D. Martin, Y. Meng, J. Santillan, and Q. Williams (2007), Equation of state and high-pressure stability of Fe<sub>3</sub>P-schreibersite: Implications for phosphorus storage in planetary cores, *Geophys. Res. Lett.*, *34*, L06302, doi:10.1029/2006GL029160.
- Seagle, C. T., A. J. Campbell, D. L. Heinz, G. Shen, and V. B. Prakapenka (2006), Thermal equation of state of Fe<sub>3</sub>S and implications for sulfur in the Earth's core, *J. Geophys. Res.*, *111*, B06209, doi:10.1029/2005JB004091.
- Shen, G., M. Rivers, Y. Wang, and S. R. Sutton (2001), Laser heated diamond cell system at the Advanced Photon Source for in situ X-ray measurements at high pressure and temperature, *Rev. Sci. Instrum.*, *72*, 1273, doi:10.1063/1.1343867.
- Stevenson, D. J., T. Spohn, and G. Schubert (1983), Magnetism and thermal evolution of the terrestrial planets, *Icarus*, *54*, 466–489, doi:10.1016/0019-1035(83)90241-5.
- Stewart, A. J., and M. W. Schmidt (2007), Sulfur and phosphorus in the Earth's core: The Fe-P-S system at 23 GPa, *Geophys. Res. Lett.*, *34*, L13201, doi:10.1029/2007GL030138.
- Stewart, A. J., M. W. Schmidt, W. van Westrenen, and C. Liebske (2007), Mars: A new core-crystallization regime, *Science*, *316*, 1323–1325, doi:10.1126/science.1140549.
- Tanaka, S. I., J. Takioto, S. K. Kwon, K. Shinoda, and S. Suzuki (2007), Lattice relaxation in Ni-P amorphous alloy accompanied with growth of Ni<sub>3</sub>P nanocrystals, *Mater. Sci. Forum*, *558–559*, 1363–1366, doi:10.4028/0-87849-443-x.1363.
- Toman, K. (1952), The structure of Ni<sub>2</sub>Si, *Acta Crystallogr.*, *5*, 329–331, doi:10.1107/S0365110X52001003.
- Walter, M., H. E. Newsom, W. Ertel, and A. Holzheid (2000), Siderophile elements in the Earth and Moon: Metal/silicate partitioning and implications for core formation, in *Origin of the Earth and Moon*, edited by R. M. Canup and K. Righter, pp. 265–289, Univ. of Ariz. Press, Tucson.
- Yupko, L. M., A. A. Svirid, and S. V. Muchnik (1986), Phase equilibria in nickel-phosphorus and nickel-phosphorus-carbon systems, *Powder Metal. Metal Ceram.*, *25*, 768–773, doi:10.1007/BF00797313.
- Zaitsev, A. I., Z. V. Dobrokhotova, A. D. Litvina, and B. M. Mogutnov (1995), Thermodynamic properties and phase equilibria in the Fe-P system, *J. Chem. Soc. Faraday Trans.*, *91*, 703–712, doi:10.1039/ft9959100703.
- 
- N. Z. Boctor, Geophysical Laboratory, Carnegie Institution of Washington, 5251 Broad Branch Road, NW, Washington, DC 20015, USA.
- L. A. Borkowski, Argonne National Laboratory, Building 434A, 9700 South Cass Avenue, Argonne, IL 60439, USA.
- P. Dera, B. Lavina, V. B. Prakapenka, M. L. Rivers, and S. R. Sutton, Center for Advanced Radiation Sources, Argonne National Laboratory, University of Chicago, Building 434A, 9700 South Cass Avenue, Argonne, IL 60439, USA. (pdera@gl.ciw.edu)
- R. T. Downs and C. T. Prewitt, Department of Geosciences, University of Arizona, 209 Gould-Simpson Building, Tucson, AZ 85721-0077, USA.